Acknowledgment

We are deeply grateful to Prof. Tetsuya Ono for his appropriate advices on mouse experiments.

This work was supported in part by a grant-in-aid from the Japan Society for the Promotion of Science, and by the Kurokawa Cancer Foundation.

References

1. Sugita, A., Sachar, D.B., Bodian, C., Ribeiro, M.B., Aufses, A.H., Jr. and Greenstein, A.J. (1991) Colorectal cancer in ulcerative colitis. Influence of anatomical extent and age at onset on colitis-cancer interval. *Gut*, 32, 167-9.

2. Kern, S.E., Redston, M., Seymour, A.B., Caldas, C., Powell, S.M., Kornacki, S. and Kinzler, K.W. (1994) Molecular genetic profiles of colitis-associated neoplasms. *Gastroenterology*, 107, 420-8.

3. Willenbucher, R.F., Aust, D.E., Chang, C.G., Zelman, S.J., Ferrell, L.D., Moore, D.H., 2nd and Waldman, F.M. (1999) Genomic instability is an early event during the progression pathway of ulcerative-colitis-related neoplasia. *Am J Pathol*, 154, 1825-30.

4. Takahashi, S., Kojima, Y., Kinouchi, Y., Negoro, K., Takagi, S., Aihara, H., Obana, N., Matsumoto, K., Hiwatashi, N. and Shimosegawa, T. (2003) Microsatellite instability and loss of heterozygosity in the nondysplastic colonic epithelium of ulcerative colitis. *J Gastroenterol*, 38, 734-9.

5. Berg, D.J., Davidson, N., Kuhn, R., Muller, W., Menon, S., Holland, G., Thompson-Snipes, L., Leach, M.W. and Rennick, D. (1996) Enterocolitis and colon cancer in interleukin-10-deficient mice are associated with aberrant cytokine production and CD4(+) TH1-like responses. *J Clin Invest*, 98, 1010-20.

6. Masumura, K., Matsui, M., Katoh, M., Horiya, N., Ueda, O., Tanabe, H., Yamada, M., Suzuki, H., Sofuni, T. and Nohmi, T. (1999) Spectra of gpt mutations in ethylnitrosourea-treated and untreated transgenic mice. *Environ Mol Mutagen*, 34, 1-8.

7. Takeiri, A., Mishima, M., Tanaka, K., Shioda, A., Ueda, O., Suzuki, H., Inoue, M., Masumura, K. and Nohmi, T. (2003) Molecular characterization of mitomycin C-induced large deletions and tandem-base substitutions in the bone marrow of gpt delta transgenic mice. *Chem Res Toxicol*, 16, 171-9.

8. Miyaki, M., Konishi, M., Kikuchi-Yanoshita, R., Enomoto, M., Igari, T., Tanaka, K., Muraoka, M., Takahashi, H., Amada, Y., Fukayama, M. and et al. (1994) Characteristics of somatic mutation of the adenomatous polyposis coli gene in colorectal tumors. *Cancer Res*,

54, 3011-20.

9. Redston, M.S., Papadopoulos, N., Caldas, C., Kinzler, K.W. and Kern, S.E. (1995) Common occurrence of APC and K-ras gene mutations in the spectrum of colitis-associated neoplasias. *Gastroenterology*, 108, 383-92.

10. O'Riordan, A. and Shanahan, F. (2001) p53 at the crossroads of colitis and cancer. *Gastroenterology*, 120, 1877-8.

11. Hussain, S.P., Amstad, P., Raja, K., Ambs, S., Nagashima, M., Bennett, W.P., Shields, P.G., Ham, A.J., Swenberg, J.A., Marrogi, A.J. and Harris, C.C. (2000) Increased p53 mutation load in noncancerous colon tissue from ulcerative colitis: a cancer-prone chronic inflammatory disease. *Cancer Res*, 60, 3333-7.

12. Noffsinger, A.E., Belli, J.M., Miller, M.A. and Fenoglio-Preiser, C.M. (2001) A unique basal pattern of p53 expression in ulcerative colitis is associated with mutation in the p53 gene. *Histopathology*, **39**, 482-92.

13. Yoshida, T., Mikami, T., Mitomi, H. and Okayasu, I. (2003) Diverse p53 alterations in ulcerative colitis-associated low-grade dysplasia:

full-length gene sequencing in microdissected single crypts. *J Pathol*, **199**, 166-75.

14. Goodman, J.E., Hofseth, L.J., Hussain, S.P. and Harris, C.C. (2004) Nitric oxide and p53 in cancer-prone chronic inflammation and oxyradical overload disease. *Environ Mol Mutagen*, **44**, 3-9

15. Souza, R.F., Lei, J., Yin, J., Appel, R., Zou, T.T., Zhou, X., Wang, S., Rhyu, M.G., Cymes, K., Chan, O., Park, W.S., Krasna, M.J., Greenwald, B.D., Cottrell, J., Abraham, J.M., Simms, L., Leggett, B., Young, J., Harpaz, N. and Meltzer, S.J. (1997) A transforming growth factor beta 1 receptor type II mutation in ulcerative colitis-associated neoplasms. *Gastroenterology*, 112, 40-5.

16. Fortune, J.M., Pavlov, Y.I., Welch, C.M., Johansson, E., Burgers, P.M. and Kunkel, T.A. (2005) Saccharomyces cerevisiae DNA polymerase delta: high fidelity for base substitutions but lower fidelity for single- and multi-base deletions. *J Biol Chem*, **280**, 29980-7.

17. Shin, C.Y., Ponomareva, O.N., Connolly, L. and Turker, M.S. (2002) A mouse kidney cell line with a G:C --> C:G transversion mutator phenotype. *Mutat Res*, **503**, 69-76.

18. Chang, C.L., Marra, G., Chauhan, D.P., Ha, H.T., Chang, D.K., Ricciardiello, L., Randolph, A., Carethers, J.M. and Boland, C.R. (2002) Oxidative stress inactivates the human DNA mismatch repair system. *Am J Physiol Cell Physiol*, 283, C148-54.

19. Hofseth, L.J., Khan, M.A., Ambrose, M., Nikolayeva, O., Xu-Welliver, M., Kartalou, M., Hussain, S.P., Roth, R.B., Zhou, X., Mechanic, L.E., Zurer, I., Rotter, V., Samson, L.D. and Harris, C.C. (2003) The adaptive imbalance in base excision-repair enzymes generates microsatellite instability in chronic inflammation. *J Clin Invest*, 112, 1887-94.

20. Kreutzer, D.A. and Essigmann, J.M. (1998) Oxidized, deaminated cytosines are a source of C --> T transitions in vivo. *Proc Natl Acad Sci U S A*, 95, 3578-82.

21. Popoff, I., Jijon, H., Monia, B., Tavernini, M., Ma, M., McKay, R. and Madsen, K. (2002) Antisense oligonucleotides to poly(ADP-ribose) polymerase-2 ameliorate colitis in interleukin-10-deficient mice. *J Pharmacol Exp Ther*, 303, 1145-54.

22. Touati, E., Michel, V., Thiberge, J.M., Wuscher, N., Huerre, M. and Labigne, A. (2003) Chronic Helicobacter pylori infections induce gastric mutations in mice. *Gastroenterology*, 124, 1408-19.

Figure legends

Figure 1. Mutation frequency of 6-TG selection in the total colon of *gpt*$^{+}$*IL-10*$^{-/-}$ mice (■) and *gpt*$^{+}$*IL-10*$^{+/+}$ mice (□). The mutation frequencies of 6-TG selection in the total colon of *gpt*$^{+}$*IL-10*$^{-/-}$ mice were significantly higher than those in the total colon of 15-weeks *gpt*$^{+}$*IL-10*$^{+/+}$ mice. $P <$ 0.05, statistically significant difference vs. *gpt*$^{+}$*IL-10*$^{+/+}$. Bars represent mean values and standard error.

Figure 2. Mutation frequency of 6-TG selection in the total colon of *gpt*$^{+}$*IL-10*$^{-/-}$ mice and *gpt*$^{+}$*IL-10*$^{+/+}$ mice (■; 15-weeks □; 40-weeks). The mutation frequencies of 6-TG selection in the total colon of *gpt*$^{+}$*IL-10*$^{-/-}$ mice were significantly higher than those in the total colon of *gpt*$^{+}$*IL-10*$^{+/+}$ mice, at 15-weeks or 40-weeks of age. The mutation frequencies of 6-TG selection in the total colon of 40-weeks *gpt*$^{+}$*IL-10*$^{-/-}$ mice were not significantly higher than those in the total colon of 15-weeks *gpt*$^{+}$*IL-10*$^{+/+}$ mice. $P < 0.05$, statistically significant difference vs. *gpt*$^{+}$*IL-10*$^{+/+}$. Bars represent mean values and standard error.

Figure 3. Mutation frequency of Spi$^-$ selection in the colon of *gpt*$^+$*IL-10*$^{-/-}$ mice (■) and *gpt*$^+$*IL-10*$^{+/+}$ mice (□). The mutation frequencies of Spi$^-$ selection in the total colon of *gpt*$^+$*IL-10*$^{-/-}$ mice were not significantly higher than those in the total colon of 15-weeks *gpt*$^+$*IL-10*$^{+/+}$ mice. $P < 0.05$, statistically significant difference vs. *gpt*$^+$*IL-10*$^{+/+}$. Bars represent mean values and standard error.

Figure 4. Mutation frequency of Spi$^-$ selection in the total colon of *gpt*$^+$*IL-10*$^{-/-}$ mice and *gpt*$^+$*IL-10*$^{+/+}$ mice (■; 15-weeks □; 40-weeks). The mutation frequencies of Spi$^-$ selection in the total colon of *gpt*$^+$*IL-10*$^{-/-}$ mice were not significantly higher than those in the total colon of *gpt*$^+$*IL-10*$^{+/+}$ mice, at 15-weeks or 40-weeks of age. The mutation frequencies of Spi$^-$ selection in the total colon of 40-weeks *gpt*$^+$*IL-10*$^{-/-}$ mice were not significantly higher than those in the total colon of 15-weeks *gpt*$^+$*IL-10*$^{+/+}$ mice. $P < 0.05$, statistically significant difference vs. *gpt*$^+$*IL-10*$^{+/+}$. Bars represent mean values and standard error.

Figure 1 Y, Sato

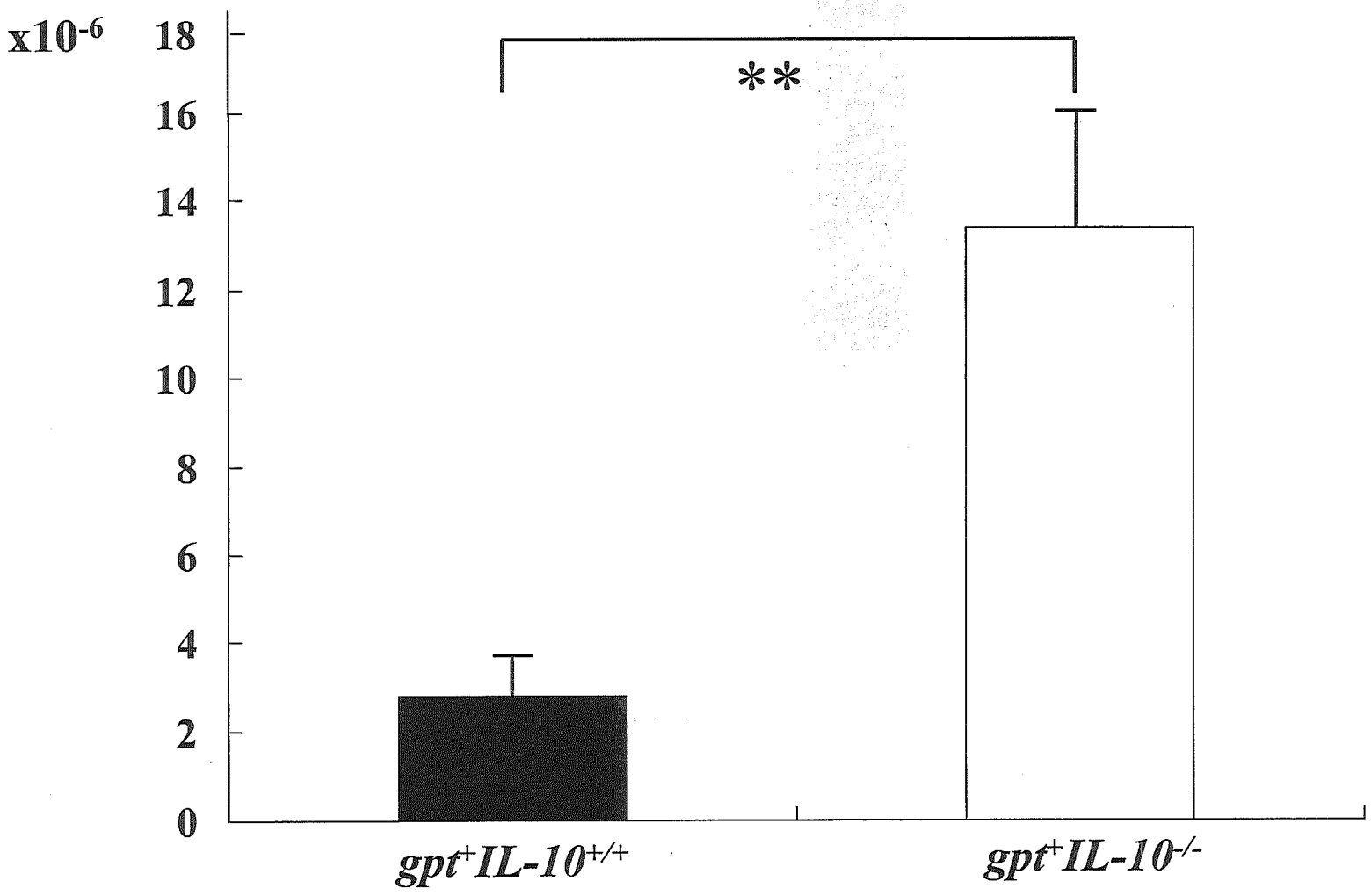

**$P<0.05$(t-test)

Figure 2　Y, Sato

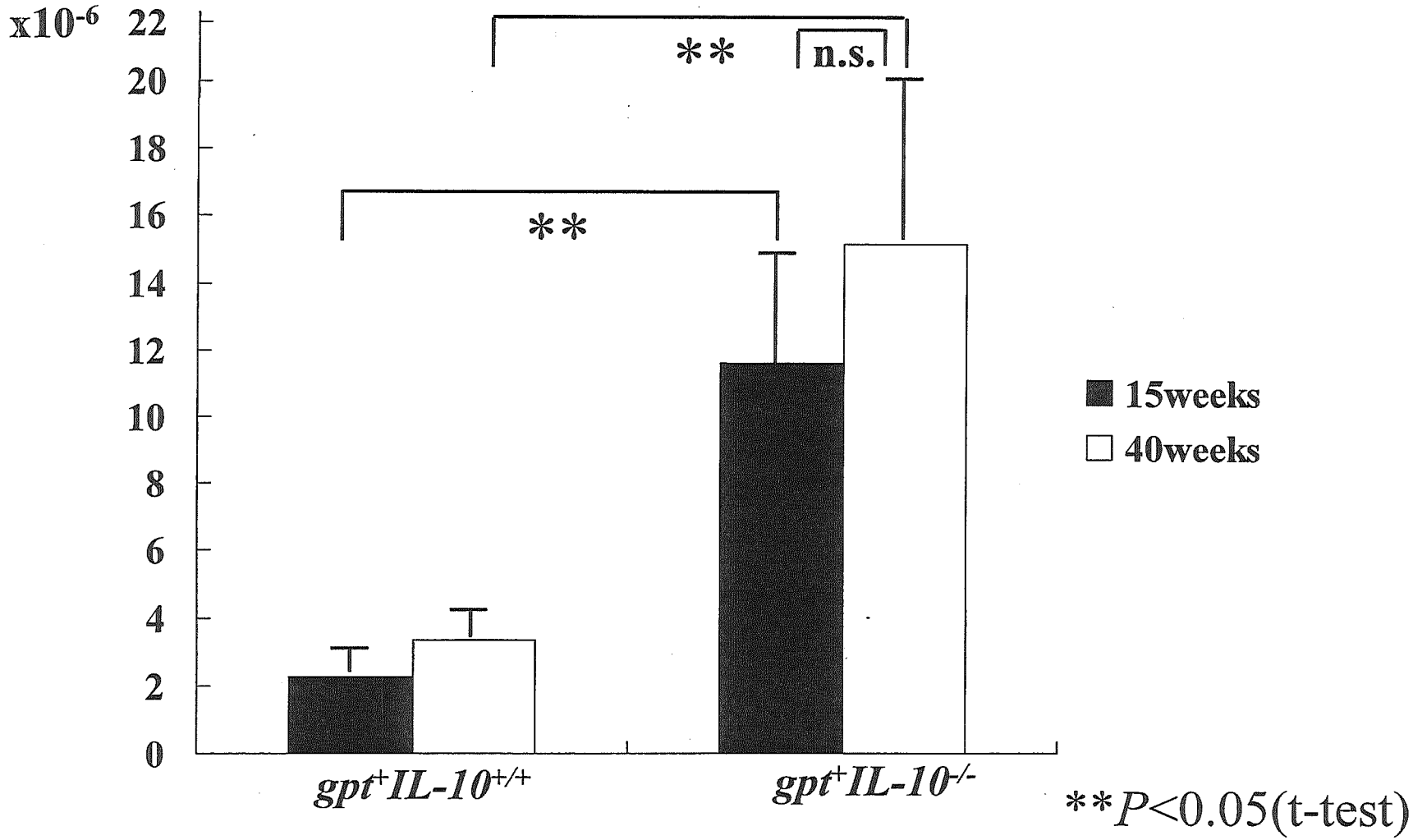

**P<0.05(t-test)

Table 1 Distribution of the different kinds of mutations in the colon(15 weeks, 6-TG selection)

	gpt $^{+}$*IL-10* $^{-/-}$			*gpt* $^{+}$*IL-10* $^{+/+}$		
	Number	**Percentage(%)**	**Mutation Frequencies(x 10^{-6})**	**Number**	**Percentage(%)**	**Mutation Frequencies(x 10^{-6})**
transition	**11**	**16.2**	**1.88**	**6**	**49.7**	**1.12**
G:C to A:T	(10)	(14.7)	(1.71)	(4)	(33.0)	(0.75)
A:T to G:C	(1)	(1.5)	(0.17)	(2)	(16.7)	(0.38)
transversion	**24**	**35.3**	**4.1**	**5**	**41.3**	**0.94**
G:C to T:A	(5)	(7.4)	(0.86)	(4)	(33.0)	(0.75)
G:C to C:G	(10)	(14.7)	(1.71)	(1)	(8.3)	(0.19)
A:T to T:A	(6)	(8.8)	(1.02)	(0)	(0)	(0)
A:T to C:G	(3)	(4.4)	(0.51)	(0)	(0)	(0)
deletion	**24**	**35.3**	**4.1**	**1**	**8.3**	**0.19**
1 bp	(24)	(35.3)	(4.1)	(1)	(8.3)	(0.19)
>2bp	(0)	(0)	(0)	(0)	(0)	(0)
insertion	**9**	**13.2**	**1.53**	**0**	**0**	**0**
total	**68**	**100**	**11.61**	**12**	**100**	**2.25**

Table 2 List of deletions or insertions in the colon(15 weeks, 6-TG selection)

gpt $^{+}$*IL-10* $^{-/-}$			*gpt* $^{+}$*IL-10* $^{+/+}$		
deletion			**deletion**		
Position	**Sequence change**	**Number**	**Position**	**Sequence change**	**Number**
283~	GGT→GG	1	315~	AAAA→AAA	1
309	-T	1			
315~	AAAA→AAA	1			
325~	CTTT→TTT	1			
332~	CCA →CC	1			
342~	AAAA→AAA	1			
348~	GG→G	3			
395~	ATA→AA	1			
414~	GTGGG→GGGG	1			
416~	GGG→GG	1			
419~	ATA→AA	1			
423~	GGG→GG	1			
431	-T	1			
438~	CCCGCC→CCCCC	4			
444~	AA→A	1			
450~	GGT→GG	4			
insertion			**insertion**		
Position	**Sequence change**	**Number**	**Position**	**Sequence change**	**Number**
256~	GTT→GTTGTT	1			
305~	AAA→AAAA	1			
325~	TTT→TTTT	1			
380~	TT→TTT	1		**Not detected**	
407~	AA→AAA	2			
416~	GGGA→GGGAA	2			

The position numbers indicate the locations where mutations were found. The numbering starts from the first nucleotide of the *gpt* gene.

Table 4 List of deletions or insertions in the colon(40 weeks, 6-TG selection)

gpt +*IL-10* -/-			*gpt* +*IL-10* +/+		
deletion			**deletion**		
Position	**Sequence change**	**Number**	**Position**	**Sequence change**	**Number**
223~	**AAA→AA**	**1**	**83~**	**AA→A**	**2**
250~	**TTCATCGTT→TTCGTT**	**1**			
308~	**TGT→TT**	**1**			
315~	**AAAA→AAA**	**1**			
423~	**GGG→GG**	**1**			
451~	**GG→G**	**1**			
insertion			**insertion**		
Position	**Sequence change**	**Number**	**Position**	**Sequence change**	**Number**
3~	**G→GG**	**1**	**264~**	**GA→GAGA**	**1**
8~	**AAAAA→AAAAAA**	**1**			
58~	**GC→GCGC**	**1**			
387~	**CCC→CCCC**	**1**			

The position numbers indicate the locations where mutations were found. The numbering starts from the first nucleotide of the *gpt* gene.

Table 3 Distribution of the different kinds of mutations in the colon(40 weeks, 6-TG selection)

	gpt $^{+}$*IL-10* $^{-/-}$			*gpt* $^{+}$*IL-10* $^{+/+}$		
	Number	**Percentage(%)**	**Mutation Frequencies(x 10^{-6})**	**Number**	**Percentage(%)**	**Mutation Frequencies(x 10^{-6})**
transition	**36**	**57.1**	**8.66**	**25**	**54.3**	**1.81**
G:C to A:T	(29)	(46)	(6.98)	(24)	(52.2)	(1.74)
A:T to G:C	(7)	(11.1)	(1.68)	(1)	(2.2)	(0.07)
transversion	**17**	**27**	**4.1**	**18**	**39.1**	**1.31**
G:C to T:A	(12)	(19)	(2.88)	(15)	(32.6)	(1.09)
G:C to C:G	(1)	(1.6)	(0.24)	(3)	(6.5)	(0.22)
A:T to T:A	(2)	(3.2)	(0.49)	(0)	(0)	(0)
A:T to C:G	(2)	(3.2)	(0.49)	(0)	(0)	(0)
deletion	**6**	**9.5**	**1.44**	**2**	**4.3**	**0.14**
1 bp	(5)	(7.9)	(1.2)	(2)	(4.3)	(0.14)
>2bp	(1)	(1.6)	(0.24)	(0)	(0)	(0)
insertion	**4**	**6.4**	**0.97**	**1**	**2.2**	**0.07**
Total	**63**	**100**	**15.17**	**46**	**100**	**3.34**

Table 5 List of mutations in the colon(15 weeks, Spi$^-$ selection)

gpt $^+$*IL-10* $^{-/-}$			*gpt* $^+$*IL-10* $^{+/+}$		
Position	**Sequence change**	**Number**	**Position**	**Sequence change**	**Number**
161~	-C	1	237	-C	1
164~	CCC→CC	1	238~	GGGG→GGG	1
226	-C	1	294	-G	1
227~	TTTTT→TTTT	2	295~	TTTTTT→TTTTT	2
235~250	-16bp	1	327	-A	2
238~	GGGG→GGG	1	333~419	-87bp	1
286~	CCCC→CCC	1	348~	CC→C	1
295~	TTTTTT→TTTTT	6	416~	TTTT→TTT	4
393~	CC→CCC	1			
416~	TTTT→TTT	2			

The position numbers indicate the locations where mutations were found. The numbering starts from the first nucleotide of the *gam* gene.

Table 6 List of mutations in the colon(40 weeks, Spi$^-$ selection)

gpt $^+$*IL-10* $^{-/-}$			*gpt* $^+$*IL-10* $^{+/+}$		
Position	**Sequence change**	**Number**	**Position**	**Sequence change**	**Number**
195~198	-TCTT	1	129	AA→A	1
227~	TTTTT→TTTT	5	227~	TTTTT→TTTT	3
232~	CC→C	3	232~	CC→C	1
238~	GGGG→GGG	2	286~	CCCC→CCC	3
277	-G	1	295~	TTTTTT→TTTTT	5
286~	CCCC→CCC	2	327	-A	1
295~	TTTTTT→TTTTT	4			
341	-T	1			

The position numbers indicate the locations where mutations were found. The numbering starts from the first nucleotide of the *gam* gene.

Genes and Environment, Vol. 28, No. 1 pp. 23-30 (2006)

Regular Article

Development of a Bacterial Hyper-sensitive Tester Strain for Specific Detection of the Genotoxicity of Polycyclic Aromatic Hydrocarbons

Masami Yamada, Keiko Matsui and Takehiko Nohmi[1]

Division of Genetics and Mutagenesis, National Institute of Health Sciences, Tokyo, JAPAN

(Received December 16, 2005; Accepted January 10, 2006)

Benzo[a]pyrene (B[a]P), one of polycyclic aromatic hydrocarbons (PAHs), is a ubiquitous environmental pollutant and a potent mutagen and carcinogen. To sensitively detect the genotoxicity of PAHs in complex mixtures extracted from environmental pollutants, *Salmonella enterica* serovar Typhimurium (*S. typhimurium*) strain YG5161 is engineered by introduction of plasmid pYG768 carrying the *dinB* gene encoding *Escherichia coli* DNA polymerase IV into standard Ames tester strain *S. typhimurium* TA1538 (Matsui *et al.*, DNA Repair in press). Strain YG5161 exhibits higher sensitivity to the genotoxicity of B[a]P and other PAHs than do strain TA1538 and TA98. As the conventional Ames tester strains do, however, strain YG5161 also detects the mutagenicity of aromatic amines and nitroaromatics with high sensitivity, which may veil the genotoxicity of PAHs in complex mixtures. *S. typhimurium* possesses strong enzyme activities of nitroreductase and *O*-acetyltransferase, which mediate the metabolic activation of aromatic amines and nitroaromatics and enhance the potent genotoxicity. In this study, we disrupted the *nfsB* and *oat* genes encoding the activation enzymes in strain TA1538 to reduce the cross sensitivity, and introduced plasmid pYG768 into the *ΔnfsBΔoat* strain. The resulting strain YG5185 retained similar high mutability to various chemicals including PAHs as did strain YG5161 and substantially decreased the sensitivity to 1-nitropyrene, 1,8-dnitropyrene and 2-amino-6-methyldipyrido[1,2-a:3′,2′-d]imidazole (Glu-P-1). We propose that the novel tester strain YG5185 is useful to specifically and sensitively detect the genotoxic PAHs in complex mixtures from various polluted environmental sources.

Key words: genotoxicity, polycyclic aromatic hydrocarbons, complex mixture, *dinB*, translesion DNA synthesis

Introduction

The ambient air and soil of urban centers and other areas can be polluted with potentially carcinogenic and genotoxic chemicals including polycyclic aromatic hydrocarbons (PAHs), most of which are emitted into the atmosphere as a result of incomplete combustion of fossil fuels associated with motor vehicles, industrial activities and home heating (1). In fact, the pollution of air and soil with PAHs is a serious problem in many countries all over the world (2). In Asia, the Chinese government assessed the state of soil contamination on the Beijing outskirts where great changes are undergoing due to the rapid urbanization and industrial development, and concluded that the pyrogenic origins, especially traffic exhausts, are the dominant sources of PAHs (3). In Korea, it is reported that typical soils from agricultural areas contained PAHs at similar level to those in soils from highly industrialized countries (4). In Japan, concentrations of particles of diameter under 1 μm with attached PAHs were measured in various locations in Tokyo and the major polluted places were main traffic roads, highways, and street tunnels (5). In Europe, 20 PAHs and 12 polychlorinated biphenyls (PCBs) in forest soils of Germany were physico-chemically determined, and PAHs were more dominantly detected than PCBs (6). In England, soil samples have been collected from the same plot in 1893, 1944 and 1987 for analysis of PAHs, and it is revealed that the surface soil had been enriched in all PAH compounds, particularly in benzo[a]pyrene (B[a]P) (7). Even in the Southern Hemisphere where pollution levels seem to be lower than those in the northern one, studies of pollution seem to be urgently necessary. In Chile, some persistent toxic substances (PTS) in soils were analyzed, which led to the conclusion that environmental PTS levels are relatively low but PAHs may be of concern in some areas of basin (8). In Brazil, Ames genotoxicity assay was carried out with and without metabolic activation for air samples at four sites in urban area, and higher mutagenic activity was identified at the sites with heavier vehicle traffic. The results using nitroreduc-

[1]Correspondence to: Takehiko Nohmi, Division of Genetics and Mutagenesis, National Institute of Health Sciences, 1-18-1 Kamiyoga, Setagaya-ku, Tokyo 158-8501, Japan. Tel: +81-3-3700-9873, Fax: +81-3-3707-6950, E-mail: nohmi@nihs.go.jp

tase- or *O*-acetyltransferase-deficient strains suggest that nitro PAHs seem to be strongly associated with the genotoxicity observed in the urban and industrial regions (9).

To sensitively detect the genotoxicity of B[a]P and other PAHs in complex mixtures extracted from various polluted environmental sources, Matsui *et al* (10). have recently engineered *Salmonella enterica* serovar Typhimurium (*S. typhimurium*) strain YG5161, which harbored plasmid pYG768 carrying *dinB* encoding *Escherichia coli* DNA polymerase IV in standard Ames tester strain TA1538. The DNA polymerase can bypass a variety of DNA lesions such as those induced by B[a]P (11,12). Thus, the expression of the polymerase enhances B[a]P-induced -2 frameshift events in CGC-GCGCG repetitive sequences in the *hisD* gene in strain TA1538, which reverse the phenotype from His^- to His^+ (13). In fact, the stain exhibits several times higher sensitivity to the genotoxicity of B[a]P than does strain TA1538 or another standard strain TA98 (10). Strain TA98 is the same as strain TA1538 but harbors plasmid pKM101 carrying *mucAB* encoding another Y-family DNA polymerase, i.e., DNA polymerase RI (14). Strain YG5161 also exhibits higher sensitivity to 10-azabenzo[a]pyrene (10-AzaB[a]P), 3-methylcholanthrene (3-MC) and 3-nitrobeno[a]pyrene (3-NB[a]P) than does strain TA1538 or TA98.

Despite the high sensitivity, strain YG5161 possesses a potential problem that is cross sensitivity to genotoxic nitroaromatics and aromatic amines. *S. typhimurium* has strong metabolic activation enzymes for nitroaromatics and aromatic amines, i.e., nitroreductase and *O*-acetyltransferase (15,16). The former is required for the reductive activation of nitroaromatics, and the latter is involved in the activation of *N*-hydroxy compounds derived from nitro- and amino-aromatics. Because of the potent enzyme activities, the genotoxicity of nitroaromatics and aromatic amines is very sensitively detected with *S. typhimurium* tester strains (17). As a consequence, the genotoxic PAHs can be veiled in complex mixtures extracted from various polluted environmental sources if genotoxic nitroaromatics or aromatic amines are contaminated.

In this study, we disrupted the *nfsB* and *oat* genes encoding nitroreductase and *O*-acetyltransferase, respectively, to decrease the cross sensitivity to nitro- and amino-aromatics. Introducing plasmid pYG768 into the *ΔnfsBΔoat* strain resulted in strain YG5185, which retained the high sensitivity to PAHs but exhibited much reduced sensitivity to nitro- and amino-aromatics. We propose that the novel strain YG5185 is useful to detect genotoxic PAHs in the complex mixtures specifically and sensitively.

Materials and Methods

Strains and plasmids: The strains and the plasmids used in this study are listed in Table 1.

Chemicals: The names, CAS registry numbers, abbreviations and sources of the chemicals assayed in this study are as follows: B[a]P (50-32-8), 7,12-dimethylbenz[a]anthracene (57-97-6, DMBA), 2-amino-6-methyldipyrido[1,2-a:3′,2′-d]imidazole (67730-11-4, Glu-P-1), and 2-aminoanthracene (613-13-8, 2-AA) from Wako Pure Chemicals (Osaka, Japan); 3-MC (56-49-5) and 1-aminoanthracene (610-49-1, 1-AA) form Sigma-Aldrich Japan K. K. (Tokyo, Japan); 1-nitropyrene (5522-43-0, 1-NP) and 1,8-dinitropyrene (42397-65-9, 1,8-DNP) from Tokyo Kasei Kogyo (Tokyo, Japan). 10-AzaB[a]P (189-92-4) and 1-nitrobenzo[a]pyrene (70021-99-7, 1-NB[a]P) were provided by Drs. Ken-ichi Saeki, Nagoya City University, Nagoya, Japan, and Kiyoshi Fukuhara, National Institute of Health Sciences, Tokyo, Japan, respectively. *N*-Ethyl-*N*′-nitro-N-nitrosoguanidine (4245-77-6, ENNG) is a laboratory stock.

Media: Luria-Bertani broth and agar were used for bacterial culture. Vogel-Bonner minimal agar plates and top agar were prepared as previously described, and used for the His^+ reversion assay with *S. typhimurium* (13). Nutrient broth (Difco, MI, U.S.A.) with ampicillin (AP, 50 μg/ml) was used for pre-cultures of strain YG5161 and YG5185 for the reversion assay.

Construction of nitroreductase deficient strain: Plasmid pYG638 (Fig. 1A) was digested with *Sal*I and *Pvu*II (New England Biolabs, MA, U.S.A.) to remove the replication origin (18), and the 6.8-kb linear *Sal*I-*Sal*I DNA fragment containing the kanamycin-resistance (Km^r) gene between two flanking regions of the *nfsB* gene was purified with JET Sorb extraction kit (Genomed GmbH, Bad. Oeynhausen, Germany) after agarose gel electrophoresis. The purified DNA fragment was treated with T4 DNA ligase (Nippon Gene, Tokyo, Japan), and introduced into *Δoat* derivative of strain TA1538, i.e., strain YG7129, by electroporation (19,20). Colonies resistant to kanamycin were selected, and replacement of the *nfsB* gene with the DNA fragment carrying the Km^r gene was examined by PCR (primers; 5′-TGGAACTGCCTTTTACCGAACACT-3′ and 5′-CCCGGACATAATAGAAAACCGGT-3′) followed by 0.8% agarose gel electrophoresis.

Mutagenicity assay: The mutagenicity assay was carried out with a pre-incubation procedure (13). Briefly, 0.1 mL overnight culture was incubated with the chemicals dissolved in 0.1 mL solvent and 0.5 mL of S9 mix for 20 min at 37°C. When S9 mix is not required, 0.5 mL of 1/15M phosphate buffer pH7.4 was added. The mixture was then poured onto agar plates with soft agar and incubated for 2 days at 37°C. Each chemical was assayed with 4–7 doses on triplicate plates with four

Table 1. Strains and plasmids used in this study

Strain	Genetic characteristic	Source
TA1538	*hisD3052, gal, Δ(chl, uvrB bio) rfa*	(13)
YG5161	the same as TA1538, but harbors pYG768; Ap^r	(10)
YG7129	the same as TA1538, but deficient in *oat*; Cm^r	(19)
YG7158	the same as YG7129, but deficient in *nfsB*; Cm^r Km^r	this study
YG5185	the same as YG7158, but harbors pYG768; Ap^r Cm^r Km^r	this study
plasmid		
pYG638	Derivative of pBR322 for the disruption of the *nfsB* gene; Km^r Ap^r (see Fig. 1)	(18)
pYG768	Derivative of pWSK29 with *dinB* gene; Ap^r	(34)

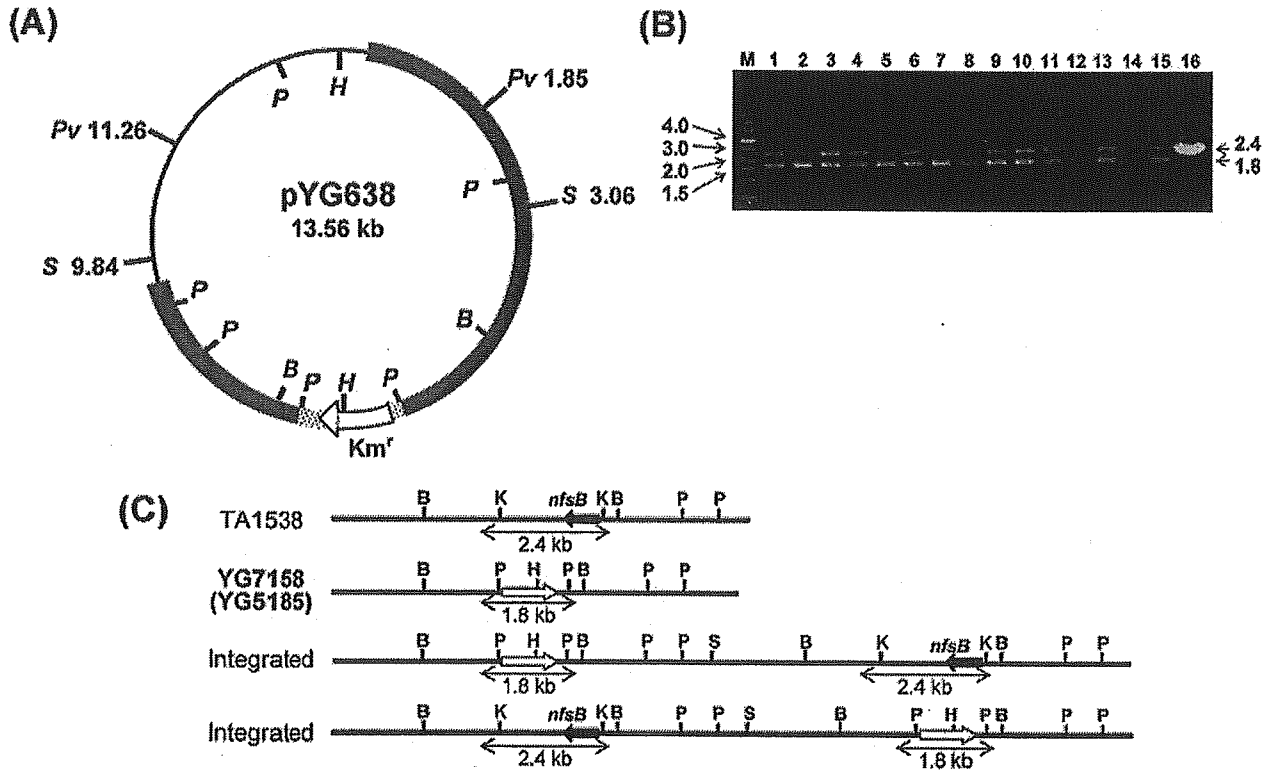

Fig. 1. Disruption of the *nfsB* gene. (A) Physical map of pYG638 (18). The thin and thick gray lines indicate DNA of plasmid pBR322 and the chromosome DNA derived from *S. typhimurium* TA1538, respectively. The dotted region shows the *Pst*I fragment derived from plasmid pUC-4k, which contains the Km^r-gene cassette, whose transcriptional direction is indicated by the arrow head. Symbols for restriction enzyme sites: B, *Bam*HI; H, *Hin*dIII; P, *Pst*I; Pv, *Pvu*II; S, *Sal*I. A *Sal*I-*Sal*I fragment containing the Km^r cassette with the size of 6.78 kb was used for targeted disruption of the *nfsB* gene by pre-ligation method. (B) Result of PCR. PCR products were subjected to 0.8% agarose gel electrophoresis. M indicates size marker and lane numbers are indicated at the top of the gel image. Lanes 2, 5, 7 and 12 indicate the clone whose *nfsB* gene has been replaced with the Km^r gene and lane 16 shows the proper size of the band including the $nfsB^+$ gene. Other lanes exhibit the clones that have the $nfsB^+$ gene as well as the Km^r-gene fragment integrated into the chromosome. (C) Partial restriction maps of the *nfsB* gene and the surrounding chromosomal region in strain TA1538 and its Km^r recombinants. Closed and open arrows indicate the position and the transcriptional direction of the *nfsB* gene and the Km^r cassette, respectively. Thin arrows indicate the size of the bands amplified by PCR in (B).

strains, i.e., TA1538, YG7158, YG5161, YG5185, in parallel.

Results

Establishment of S. typhimurium strain YG5185: To reduce the cross sensitivity to aromatic amines and nitroaromatics, we disrupted the *nfsB* gene of *S. typhimurium* strain YG7129, which is the same as strain TA1538 but the *oat* gene is already disrupted (Table 1). After electroporation of the DNA fragments containing the Km^r gene instead of the *nfsB* gene into strain YG7129, Km^r colonies were selected. Chromosome